 Related Commentary, page 1205

# Hemoglobin-driven pathophysiology is an in vivo consequence of the red blood cell storage lesion that can be attenuated in guinea pigs by haptoglobin therapy

Jin Hyen Baek,[1] Felice D'Agnillo,[1] Florence Vallelian,[2] Claudia P. Pereira,[1] Matthew C. Williams,[1] Yiping Jia,[1] Dominik J. Schaer,[2,3] and Paul W. Buehler[1]

[1]Laboratory of Biochemistry and Vascular Biology, Division of Hematology, Center for Biologics Evaluation and Research (CBER), FDA, Bethesda, Maryland, USA. [2]Division of Internal Medicine and Division of Clinical Immunology, University Hospital, Zurich, Switzerland. [3]Center of Evolutionary Medicine and Center for Integrative Human Physiology, University of Zurich, Zurich, Switzerland.

**Massive transfusion of blood can lead to clinical complications, including multiorgan dysfunction and even death. Such severe clinical outcomes have been associated with longer red blood cell (rbc) storage times. Collectively referred to as the rbc storage lesion, rbc storage results in multiple biochemical changes that impact intracellular processes as well as membrane and cytoskeletal properties, resulting in cellular injury in vitro. However, how the rbc storage lesion triggers pathophysiology in vivo remains poorly defined. In this study, we developed a guinea pig transfusion model with blood stored under standard blood banking conditions for 2 (new), 21 (intermediate), or 28 days (old blood). Transfusion with old but not new blood led to intravascular hemolysis, acute hypertension, vascular injury, and kidney dysfunction associated with pathophysiology driven by hemoglobin (Hb). These adverse effects were dramatically attenuated when the high-affinity Hb scavenger haptoglobin (Hp) was administered at the time of transfusion with old blood. Pathologies observed after transfusion with old blood, together with the favorable response to Hp supplementation, allowed us to define the in vivo consequences of the rbc storage lesion as storage-related posttransfusion hemolysis producing Hb-driven pathophysiology. Hb sequestration by Hp might therefore be a therapeutic modality for enhancing transfusion safety in severely ill or massively transfused patients.**

## Introduction

Donor-derived red blood cell (rbc) products are routinely stored for up to 42 days before transfusion. Retrospective and prospective analyses of patients undergoing multiple blood transfusions have correlated poor clinical outcome to the number of older storage blood units received (1–3). This may be particularly relevant for massive transfusion that is arbitrarily defined by replacement of the total blood volume (approximately 10 units) in 24 hours or acute administration of greater than half the blood volume per hour (4). However, the causes for observed adverse outcomes are not clear.

Multiple biochemical changes that occur to rbc during storage are collectively referred to as the rbc storage lesion. These changes include alterations in oxygen binding and oxidative damage as well as complex architectural changes in the rbc membrane and/or cytoskeleton that result in increased fragility. Reduced rbc deformability with storage time correlated with decreased rbc survival in vivo (5) and may be accompanied by enhanced lysis of donor rbc with intravascular hemolysis after transfusion. Normal and disease state rodent models have suggested that transfusion of older blood increases senescent rbc clearance (6), iron-induced inflammation (7, 8), and tissue oxygen debt due to microcirculatory derangement (9), potentially caused by microcirculatory rbc trapping (10).

Cell-free hemoglobin-driven (Hb-driven) reactions contribute to the pathophysiology of genetic and acquired hemolytic anemia (11–15). The main physiologic effects of free Hb in these conditions are related to vascular dysfunction and heme-driven oxidative reactions. Extracellular Hb has also been suggested as a causative factor that contributes to adverse clinical events after transfusion of stored rbc (16, 17). A previous prospective evaluation of trauma patients in Japan revealed that whole blood transfusion of more than 2,000 ml resulted in elevated free Hb as well as haptoglobin (Hp) consumption, indicating significant intravascular lysis of donor rbc after transfusion (18). Moreover, mean blood storage time was positively correlated with the appearance of serum Hb and negatively correlated with serum Hp concentrations (18).

The vasculature and kidney are heavily exposed to Hb during intravascular hemolysis (19). Therefore, in this study, we hypothesize that the rbc storage lesion may be defined in vivo by intravascular Hb release that may finally alter renal and vascular homeostasis and thereby promote adverse outcomes caused by transfusion of stored blood. We also hypothesize that the circulatory sequestration of Hb by Hp coinfusion could prevent adverse consequences of older stored-blood transfusion (20).

To test these hypotheses, we evaluated a guinea pig model of massive blood transfusion. The choice of the guinea pig as a relevant species to study blood transfusion–related pathologies in vivo was previously suggested (21, 22). Guinea pig rbc contain single variant Hb, unlike rats or mice, and are dependent on 2,3-diphos-

**Conflict of interest:** The authors have declared that no conflict of interest exists.
**Citation for this article:** *J Clin Invest.* 2012;122(4):1444–1458. doi:10.1172/JCI59770.

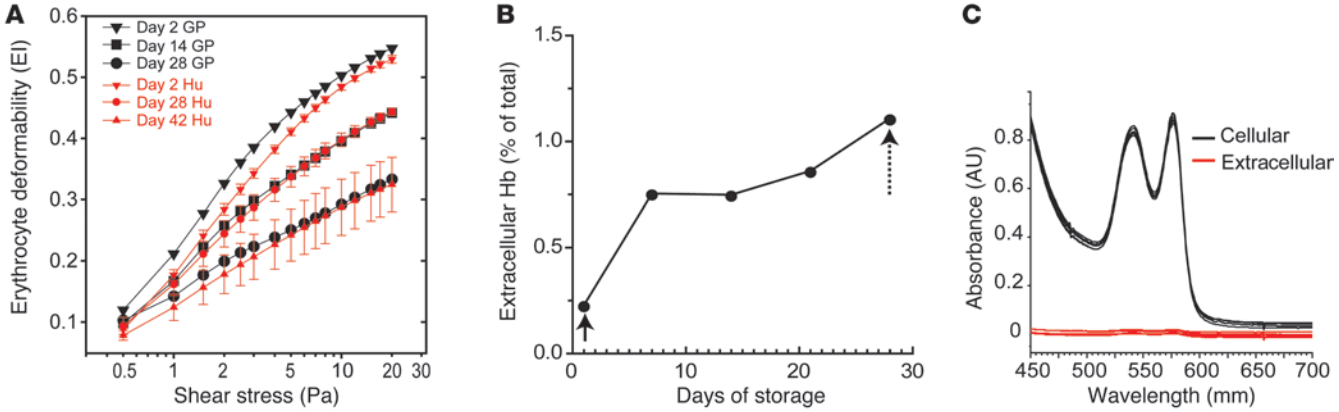


**Figure 1**

In vitro deformability of stored rbc. (**A**) Shear stress versus EI plots for guinea pig (GP) rbc collected and stored in CPDA-1/AS-3 at days 2, 14, and 28 of storage. The corresponding plots for human (Hu) cells collected and stored in CPDA-1/SAG-M for 2, 28, and 42 days are shown for comparison. (**B**) The percentage of free Hb in transfused cell supernatant over storage time. The initial measurements made after leukocyte reduction (solid arrow) and prior to transfusion (dotted arrow) are shown over time and are within the regulatory limits for human transfusion. (**C**) UV-visible spectra of intracellular and extracellular Hb at day 28 of storage.

phoglycerate, unlike bovine or ovine species (23). Additionally, as they do not produce ascorbate, guinea pigs are relevant species to evaluate the physiologic effects of Hb oxidation (24, 25).

This study provides evidence for acute adverse events after older blood transfusion in the vasculature and kidney that are consistent with free Hb–mediated processes. Therapeutic Hp administration did not halt intravascular rbc destruction per se but was highly effective at preventing hemolysis-related pathologies. Our data suggest that, on a physiologic level, after massive transfusion, the storage lesion is ultimately determined by in vitro membrane changes that contribute to hemolysis in vivo. Moreover, these effects can be addressed with therapeutic modalities to bind and sequester Hb during blood transfusion.

## Results

*Deformability of transfused rbc and in vitro hemolysis*. The elongation index (EI) of rbc was evaluated as a species-independent quantitative surrogate marker of the structural changes that occur during storage. Guinea pig rbc stored from 0 to 28 days were evaluated over a range of shear stresses from 0–20 Pa by osmotic gradient ektacytometry. The EI of guinea pig rbc at maximum shear stress was decreased by 12% over 14 days of storage and by 31% over 28 days of storage. Ektacytometry of human stored rbc is shown as EI compared with shear stress on days 2, 28, and 42 (Figure 1A). Data indicate that under approved storage conditions for 42 days human and guinea pig rbc show similar responses to osmotic stress on day 2. While, membrane rigidity increased at differing rates, human storage at day 28 was comparable to guinea pig storage day at 14, and human storage at day 42 was comparable to guinea pig storage at day 28 (Figure 1A). As a result, in our model, guinea pig blood stored for 28 days was determined acceptable to approximate human blood stored for 42 days (referred to herein as old blood), and guinea pig blood stored for 21 days was evaluated for the purposes of elucidating temporal storage-dependent effects in vivo. The mean accumulation of extracellular Hb from in vitro hemolysis during storage increased from 0.41 mg/ml (0.22% of the total Hb) after leukocyte reduction to 1.50 mg/ml (~1.0% of the total Hb) at the time of transfusion (Figure 1B).

*Transfusion of longer-term storage rbc leads to sustained intravascular hemolysis*. The extent of hemolysis in the different treatment groups after 80% transfusion was followed for 24 hours to evaluate (a) hematocrit (Hct), (b) plasma Hb, and (c) size-exclusion chromatography of Hp-sequestered plasma Hb. Basal Hct in treatment groups was 35.6% ± 1.2% blood after 2 days of storage (referred to herein as new blood), 34.0% ± 0.82% old blood, and 37.3% ± 0.82% old blood plus Hp. Similar to basal levels, 24-hour Hct was 35.4% ± 1.71% after new-blood transfusion. Old blood (with or without Hp) transfusion resulted in a significant ($P < 0.05$, compared with new blood and baseline) Hct reduction of 8.3% (29.0% ± 2.42%) and 6% (28.0% ± 2.18%), respectively (Figure 2A). Pooled plasma from the new blood group showed no Hb accumulation relative to nontreated animals (NTs) (Figure 2B). In contrast, significant plasma Hb accumulated after old-blood transfusion with and without Hp coinfusion. Interestingly, Hb released in the old blood group was bright red (Figure 2B) or predominantly in the ferrous Hb ($HbFe^{2+}$) form (86%), with mean area under the curve from 0 to 24 hours ($AUC_{0–24h}$) values for total Hb, $HbFe^{2+}$, and ferric Hb ($HbFe^{3+}$) equal to 4,567 $\mu M \cdot h \cdot ml^{-1}$, 3,911 $\mu M \cdot h \cdot ml^{-1}$, and 656.5 $\mu M \cdot h \cdot ml^{-1}$, respectively. This result suggested an ongoing level of hemolysis, coupled with rapid extravascular distribution and clearance over the 24-hour evaluation period (Figure 2C). Conversely, Hp coadministration led to Hb-Hp complex formation after transfusion, and, as a result of the much longer half-life of the complex compared with that of free Hb, the heme-oxidized Hb-Hp complex did accumulate over time (Figure 2D). The half-life of the complex is prolonged compared with the short half-life of free Hb because renal filtration of Hb (which is responsible for the rapid elimination of non-Hp-bound Hb) is blocked. Additionally, saturation of the CD163-related macrophage Hb-Hp clearance system by supraphysiological levels of Hb-Hp complex may lead to its accumulation within the circulation and delay elimination from plasma in our model. This was demonstrated by a darker red/brown color in plasma (Figure 2B), indicative of increased $HbFe^{3+}$ (38%) as well as increased circulating total Hb-Hp ($AUC_{0–24h}$ = 31,464 $\mu M \cdot h \cdot ml^{-1}$), $HbFe^{2+}$-Hp ($AUC_{0–24h}$ = 19,388 $\mu M \cdot h \cdot ml^{-1}$), and

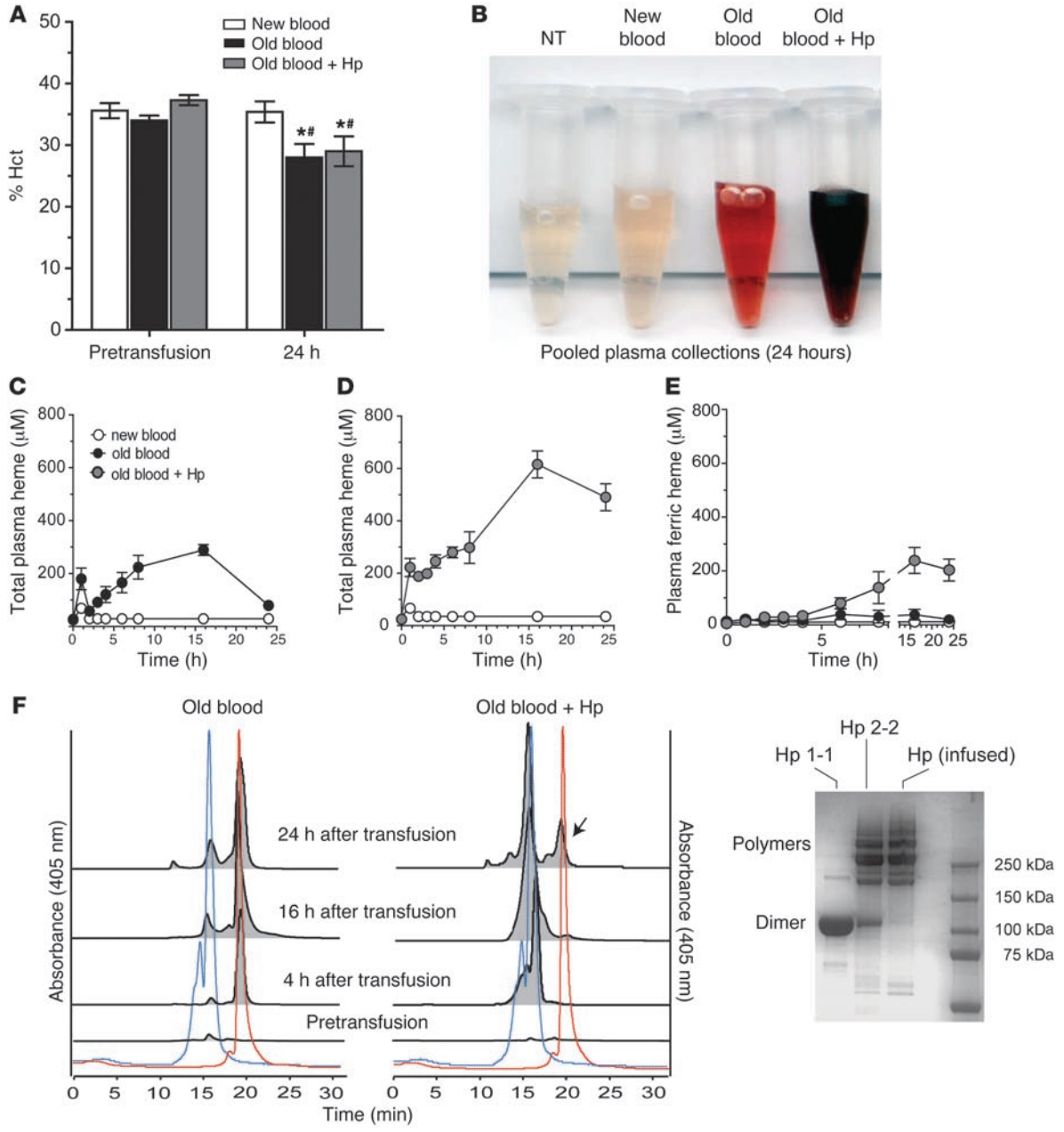


**Figure 2**

In vivo Hb exposure after blood transfusion with or without Hp. (**A**) The percentage Hct did not differ among groups immediately prior to transfusion ($P > 0.05$). Animals transfused with old blood with or without Hp demonstrated small but significantly decreased Hct levels over the 24 hours after transfusion compared with their own groups baseline ($^*P < 0.05$) and new-blood transfusion at 24 hours ($^\#P < 0.05$). (**B**) Aliquot of pooled plasma obtained over the 24-hour collection period. (**C**) Plasma Hb as total heme concentrations over time compared with new blood. (**D**) Plasma Hb as total heme after old-blood transfusion plus Hp coinfusion. (**E**) The contribution of $HbFe^{3+}$ or met-heme accumulation in plasma over time. The $AUC_{0–24h}$ values are described in the Results, with $AUC_{0–24h}$ for old blood transfusion, with or without Hp, greater than that for new blood ($P < 0.05$), and $AUC_{0–24h}$ for old blood plus Hp transfusion greater than that for old blood ($P < 0.05$). (**F**) Distribution between free Hb and Hp-bound Hb (Hb-Hp complex) in plasma over 24 hours evaluated by size-exclusion chromatography of plasma. The red and blue dotted lines represent Hb and Hb-Hp standards, respectively. Representative samples at 4, 16, and 24 hours indicate free Hb after old-blood transfusion and Hp-bound Hb after old blood plus Hp transfusion. The arrow indicates the presence of free Hb by 24 hours in the old blood plus Hp group. The distribution of standard Hp isoforms 1-1 and 2-2 and infused Hp is shown.

$HbFe^{3+}$-Hp ($AUC_{0–24h}$ = 12,076 μM·h·ml$^{-1}$). The accumulation of $HbFe^{3+}$-Hp over time is shown in Figure 2E. Further confirmation of circulatory Hb-Hp complex formation after old blood administration (with or without Hp) is demonstrated by size-exclusion chromatography of plasma prior to and at 4, 16, and 24 hours after transfusion (Figure 2F). Data demonstrate that old-blood transfusion without Hp coadministration leads to cell-free Hb in plasma over a 24-hour period (chromatography peak

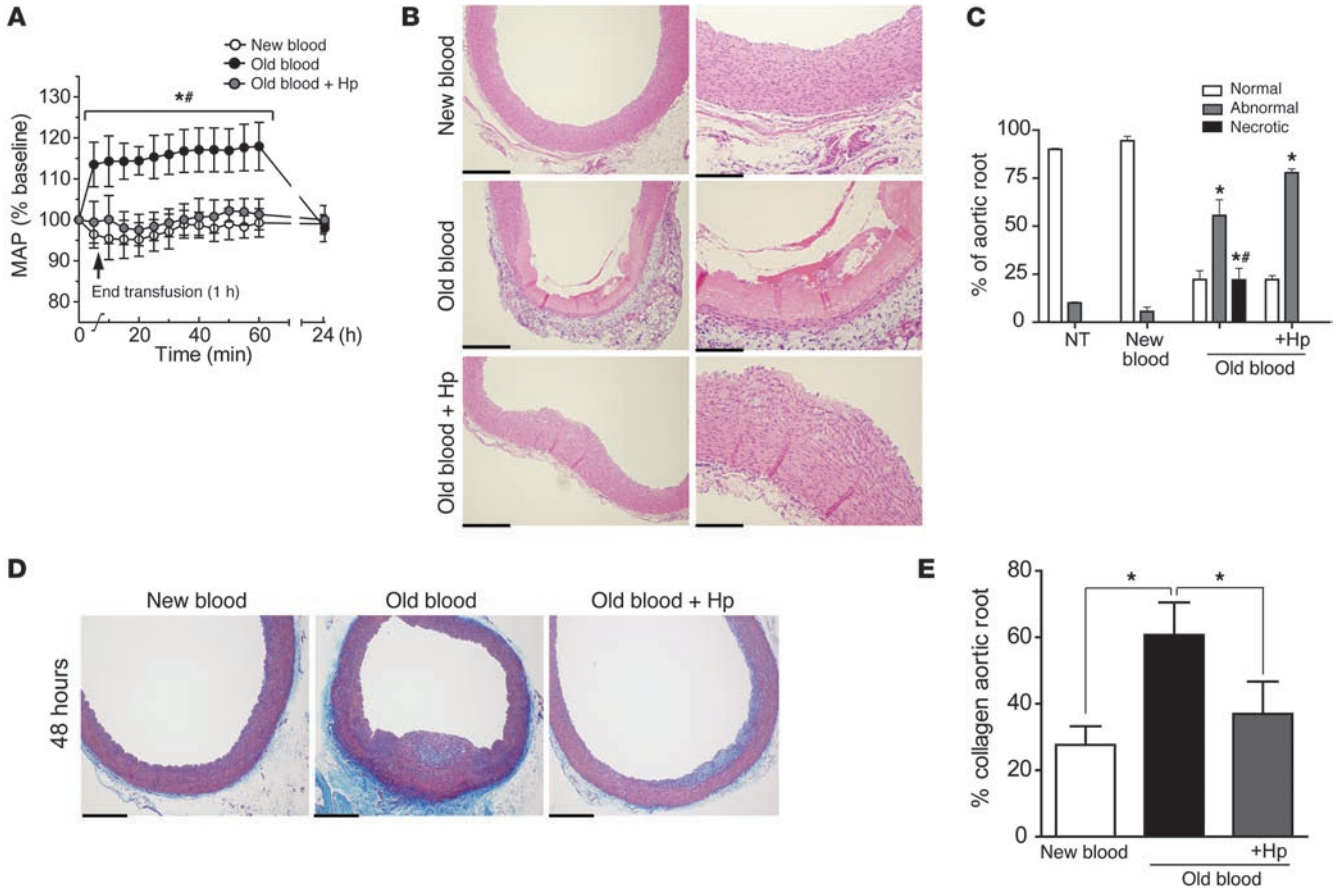


**Figure 3**

Transfusion-related vascular changes. (**A**) Acute mean arterial pressure (MAP) changes observed after transfusion of new, old, and old blood plus Hp. Significant increases in mean arterial pressure were observed after old blood transfusion compared with those after transfusion of new blood and old blood plus Hp, which were not different than basal levels. (**B**) Vascular changes in H&E-stained sections of the aortic root harvested 24 hours after transfusion. New-blood transfusion at 24 hours indicates no pathological changes, and old-blood transfusion at 24 hours indicates extensive luminal to medial coagulative necrosis, while Hp coinfusion attenuates the effects of old blood. Original magnification, ×200 (**B**, left); ×400 (**B**, right). (**C**) The percentage of normal (white bars), abnormal (gray bars), or necrotic (black bars) aortic root. (**D**) Abnormal and necrotic regions of the aortic root demonstrated collagen deposits in the vascular wall 48 hours after transfusion. Original magnification, ×100. (**E**) Old blood had a significantly greater percentage of collagen deposition compared with new and old blood plus Hp. Scale bars (1 cm) = 50 μm (**B**, left); 25 μm (**B**, right); 100 μm (**D**). $^{*}P < 0.05$; $^{\#}P < 0.05$.

coeluting with Hb standard at 18.5 minutes, 405 nm). Conversely, coadministration of Hp with old blood captured Hb within a Hb-Hp complex (chromatography peaks coeluting with Hb-Hp standard at 13.5 to 15 minutes, 405 nm). By 24 hours, a small free Hb peak was detectable in most plasma samples, indicating the beginning of oversaturation of coinfused Hp. Transfusion of new blood demonstrated a small total plasma Hb exposure over the 24-hour collection period ($AUC_{0-24h}$ = 73.4 $\mu M \cdot h \cdot ml^{-1}$), which appears to be attributable to the initial period of transfusion.

*Stored rbc transfusion induces functional and structural vascular changes that are attenuated by Hp coadministration.* The vasculature is the first organ system exposed to Hb, degradation products of rbc lysis, and to Hb-Hp complexes. Exposure to free Hb is known to elicit an increase in blood pressure (20, 26). Hb exposures have also been associated with cardiovascular toxicity in certain species, manifested as early-onset (within 24 hours) myocardial lesions (27). Therefore, we examined the vascular effects of new and older storage blood transfusion with or without Hp.

This study demonstrates that new-blood transfusion does not alter baseline systolic (70.1 ± 1.2 mmHg), diastolic (45.7 ± 5.1 mmHg), or mean (53.8 ± 0.54 mmHg) arterial blood pressure. Conversely, old blood transfusion significantly increased ($P < 0.05$) systolic (23.4% ± 10.5%), diastolic (14.7% ± 5.64%), and mean (17.9% ± 5.87%) arterial blood pressure over basal values. This effect was transient (1–2 hours); however, the coadministration of Hp with old-blood transfusion attenuated the blood pressure response to that observed at baseline and with new blood administration (Figure 3A).

Previous work has suggested a strong association between Hb and NO in blood pressure regulation during hemolytic states (16, 28, 29). Our data are in general agreement with the NO depletion hypothesis; however, our comparative analysis of plasma NO consumption, NO metabolite plasma levels, blood pressure, and vascular damage over time as well as across different treatment groups (old blood with or without Hp) suggest a dissociation among these parameters (Supplemental

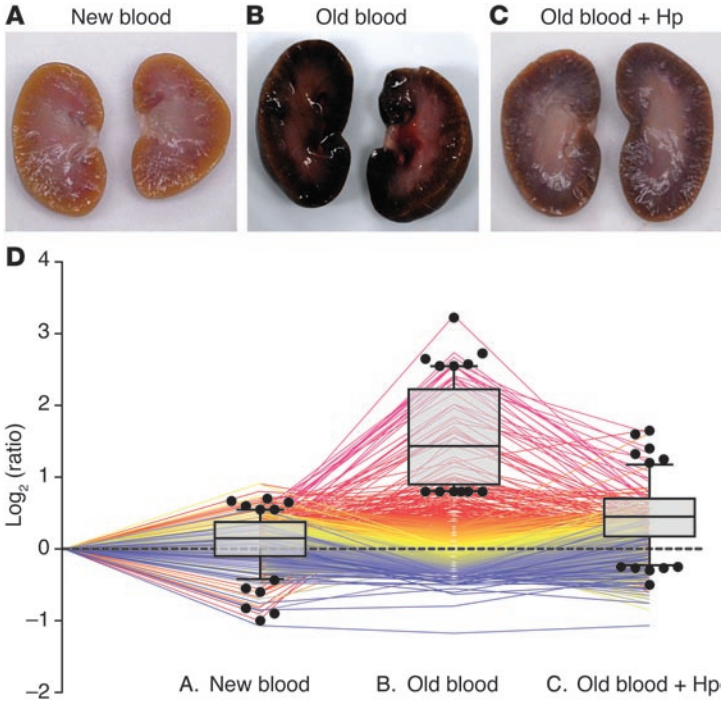


**Figure 4**
Initial tissue screening — gross pathology and proteomic profiling. (**A**–**C**) Gross morphologic changes in kidneys of animals transfused with (**A**) new blood, (**B**) old blood, and (**C**) old blood plus Hp at 24 hours. (**D**) All proteins that were identified/quantified in at least 2 out of 4 experiments are shown as color-coded lines that represent the relative abundance across the 3 treatment conditions (compared with nontreated [represented by the dotted line]). The proteins that were identified as overrepresented (>2 SD) in animals transfused with old blood are shown in the box plot overlay. Each symbol represents an individual animal. Box plots represent 25%, 50%, and 75% percentiles, horizontal bars represent median values, and whiskers indicate 10% to 90% percentiles.

Figures 5 and 6; supplemental material available online with this article; doi:10.1172/JCI59770DS1). Plasma from animals transfused with old blood with or without Hp demonstrated equal NO consumption at 1 hour after transfusion (Supplemental Figure 5A). At this time point, the maximal hypertensive response was observed in the animals transfused with old blood, but no blood pressure changes occurred in the Hp coinfusion group. In parallel with continuous Hb accumulation over time, NO consumption activity of plasma did increase, and significantly more NO consumption was measured with plasma sampled at 24 hours after transfusion (Supplemental Figure 5A) when blood pressure values approximated baseline. These ex vivo data are supported in vivo by the finding that NO metabolites decreased over time in all animal groups that were transfused with old blood and dose escalations of Hp (Supplemental Figure 5B), regardless of the presence or absence of a transient blood pressure response (Supplemental Figure 5C). In agreement with these findings, stopped flow kinetic data demonstrated nearly identical second-order rate constants for the dioxygenation reaction of oxy-Hb ($k'_{ox}$, NO = 18.8 $\mu M^{-1}s^{-1}$) and oxy-Hb-Hp ($k'_{ox}$, NO = 15.9 $\mu M^{-1}s^{-1}$) (Supplemental Figure 5D). The second-order rate constants for NO binding to met-Hb ($k'_{NO(Fe3+)}$ = 6.9 × $10^3$ $M^{-1}s^{-1}$) and met-Hb-Hp ($k'_{NO(Fe3+)}$ = 6.8 × $10^3$ $M^{-1}s^{-1}$) were also found to be similar (Supplemental Figure 5E). The effects of old blood plus increasing Hp doses on vascular changes are shown in Supplemental Figure 6. Taken together, the vascular protective activity of Hp treatment cannot be explained by a simple biochemical mechanism that would involve attenuated NO reactivity of the complex.

To explore other factors that may contribute to acute blood pressure attenuation after older blood administration, we analyzed Hb and Hb-Hp oxidative states over time in our model. Attenuation of Hb-induced blood pressure response has been suggested in reports that show that oxidized ($Fe^{3+}$) Hb is associated with increased viscosity (30) and decreased reactivity with NO (31). In Hp-treated animals, oxidized Hb ($Fe^{3+}$) in the Hb-Hp complex began to accumulate in the plasma at 8 hours, 138 ± 3.00 μM (38% of total), and reached a maximum of 239 ± 48.0 μM (45% of total) at 16 hours (Figure 2E). However, within the critical early time period after transfusion, when a hypertensive response can be observed in the non-Hp-treated animals, there was apparently no excess of $Fe^{3+}$ Hb in the Hp-treated animals.

In this study, the root of the aortic arch was evaluated for transfusion-related injury. New-blood transfusion did not show abnormal changes in aorta (Figure 3, B–E). However, old-blood transfusion was associated with coagulative necrosis, in some animals extending from the luminal tunica intima to deep within the tunica media (Figure 3, B–E). This observation was attenuated by Hp coinfusion with old blood (Figure 3, B–E). Iron deposition was observed in the perivascular regions around the vasa vasorum supplying the aortic tunica adventitia and within the connective tissue after transfusion with old blood with or without Hp but not after transfusion with new blood (Supplemental Figure 4, A–C). Regions containing iron also showed colocalized immunoreactivity for HO-1 and CD163, which indicates the accumulation of peripheral blood monocytes/macrophages (Supplemental Figure 4, A–C). Taken together, these observations suggest that Hb exposure resulting from in vivo hemolysis may play a causative role in the vascular abnormalities observed after old-blood transfusion and that Hp could be effective at limiting vascular toxicity despite the increased circulation time of the Hb-Hp complex. To explore the Hp dose-dependent protective effect, we evaluated attenuation of vascular (aortic root) injury after transfusion of old blood with Hp at doses of 100 mg, 300 mg, and 900 mg (Supplemental Figure 6A). The response to increasing Hp doses was quantified by histopathological scoring of aortic root sections (Supplemental Figure 6B). Our data indicate a general improvement in old blood–induced aortic root injury with increasing Hp dose. Images in Supplemental Figure 6A show

**Table 1**
Quantitative analysis of the kidney proteome of animals transfused with new blood, old blood, and old blood plus Hp relative to the tissue proteome of untreated guinea pigs

| Protein name | kDa | New blood (fold enrichment) | Old blood (fold enrichment) | Old blood plus Hp (fold enrichment) | *n* | Functional category |
|---|---|---|---|---|---|---|
| Hb-β | 16 | 0.18 ± 0.59 | 3.23 ± 0.59 | 0.60 ± 0.57 | 4 | Heme/ox |
| Hb-α | 15 | 0.10 ± 0.27 | 2.73 ± 0.99 | 0.78 ± 0.32 | 4 | Heme/ox |
| Citron Rho-interacting kinase | 135 | 0.20 ± 0.14 | 2.65 ± 1.06 | 0.80 ± 0.00 | 2 | |
| Serum amyloid A-4 | 14 | 0.25 ± 0.47 | 2.58 ± 0.42 | 1.33 ± 0.46 | 4 | Tubulus reabsorbed |
| Thrombospondin-4 | 103 | 0.50 ± 0.26 | 2.53 ± 0.49 | 0.93 ± 0.86 | 3 | Tubulus reabsorbed |
| Pigment epithelium derived | 46 | 0.30 ± 0.17 | 2.53 ± 0.93 | 0.70 ± 0.17 | 3 | Tubulus reabsorbed |
| Cystatin-C | 16 | 0.28 ± 0.15 | 2.53 ± 0.34 | 0.98 ± 0.61 | 4 | Tubulus reabsorbed |
| Complement factor D | 28 | 0.48 ± 0.57 | 2.40 ± 0.49 | 1.60 ± 0.58 | 4 | Tubulus reabsorbed |
| Myosin light chain 1 | 17 | 0.00 ± 0.14 | 2.40 ± 0.99 | 0.15 ± 0.64 | 2 | |
| Heme oxygenase 1 | 32 | 0.30 ± 0.36 | 2.37 ± 0.67 | 1.20 ± 1.25 | 3 | Heme/ox (Nrf-2) |
| Apolipoprotein E | 34 | 0.38 ± 0.35 | 2.35 ± 0.38 | 0.68 ± 0.34 | 4 | Tubulus reabsorbed |
| Ferritin light chain | 20 | 0.38 ± 0.22 | 2.30 ± 0.70 | 1.40 ± 0.68 | 4 | Heme/ox |
| SPARC | 35 | 0.05 ± 0.07 | 2.30 ± 0.71 | 0.45 ± 0.64 | 2 | |
| Thrombospondin-1 | 130 | 0.55 ± 1.63 | 2.15 ± 0.92 | 0.45 ± 0.21 | 2 | |
| Angiotensinogen | 53 | 0.03 ± 0.05 | 2.00 ± 0.65 | 1.08 ± 0.33 | 4 | |
| Trypsin inhibitor H4 | 105 | –0.03 ± 0.21 | 2.00 ± 0.46 | 0.73 ± 0.49 | 3 | |
| Dystroglycan | 96 | 0.30 ± 0.42 | 2.00 ± 0.85 | 0.30 ± 0.71 | 2 | |
| $\beta_2$ microglobulin | 14 | 0.15 ± 0.31 | 1.83 ± 0.22 | 0.98 ± 0.67 | 4 | Tubulus reabsorbed |
| Lactotransferrin | 71 | –0.05 ± 0.07 | 1.80 ± 0.57 | 0.20 ± 0.28 | 2 | Tubulus reabsorbed |
| Ferritin heavy chain | 21 | 0.20 ± 0.14 | 1.75 ± 0.21 | 1.25 ± 0.49 | 2 | Heme/ox |
| Prothrombin | 70 | –0.20 ± 0.28 | 1.70 ± 0.57 | –0.10 ± 0.00 | 2 | Tubulus reabsorbed |
| Integral membrane protein 2B | 26 | 0.10 ± 0.00 | 1.65 ± 0.21 | 0.25 ± 0.49 | 2 | |
| Gelsolin | 81 | 0.05 ± 0.13 | 1.63 ± 0.36 | 0.43 ± 0.43 | 4 | |
| Retinol-binding protein 4 | 23 | 0.23 ± 0.17 | 1.60 ± 0.47 | 0.53 ± 0.51 | 4 | Tubulus reabsorbed |
| Collagen α-1 | 178 | 0.40 ± 0.50 | 1.60 ± 0.26 | 0.37 ± 0.64 | 3 | |
| Fibulin-1 | 76 | 0.33 ± 0.25 | 1.53 ± 0.35 | 0.57 ± 0.51 | 3 | |
| Vitamin D–binding protein | 53 | –0.30 ± 0.10 | 1.43 ± 0.35 | 0.50 ± 0.56 | 3 | Tubulus reabsorbed |
| Thioredoxin peroxidase | 22 | –0.05 ± 0.26 | 1.28 ± 0.43 | 0.03 ± 0.38 | 4 | Heme/ox (Nrf-2) |
| Protein S100-A9 (MRP-14) | 14 | –0.43 ± 0.64 | 1.23 ± 0.12 | –0.27 ± 0.12 | 3 | |
| Complement factor B | 86 | –0.27 ± 0.21 | 1.20 ± 0.40 | 0.27 ± 0.91 | 3 | Tubulus reabsorbed |
| MIZ domain protein 1 | 116 | 0.65 ± 0.07 | 1.20 ± 0.28 | 1.65 ± 0.21 | 2 | |
| Apolipoprotein D | 22 | –0.25 ± 0.49 | 1.15 ± 0.07 | 0.55 ± 0.21 | 2 | Tubulus reabsorbed |
| Biliverdin reductase | 22 | 0.00 ± 0.08 | 1.05 ± 0.24 | 0.33 ± 0.21 | 4 | Heme/ox |
| Complement C3 | 103 | –0.23 ± 0.29 | 1.05 ± 0.33 | 0.25 ± 0.17 | 4 | Tubulus reabsorbed |
| Fibrinogen A | 62 | –0.83 ± 0.54 | 1.00 ± 0.65 | –0.25 ± 0.47 | 4 | Tubulus reabsorbed |
| Kininogen-1 | 46 | –0.20 ± 0.26 | 1.00 ± 0.56 | 0.13 ± 0.55 | 3 | Tubulus reabsorbed |

The top hits with highest abundance ratios of old blood–transfused animals versus control animal tissues are shown. (Supplemental Table 1 includes complete proteome analysis data.) SPARC, secreted protein acidic and rich in cysteine; Heme/ox, Hb exposure/oxidative stress response.

representations of normal, abnormal, and coagulative necrotic vascular tissue from representative groups. As shown in Supplemental Figure 6B, nontransfused animals and animals transfused with new blood demonstrated 90%–95% normal aortic root vasculature. Conversely, transfusion with old blood demonstrated 22% ± 4.5% (normal), 56% ± 8.2% (abnormal), and 22% ± 6.0% (necrotic) regions. This was unchanged with a 100 mg dose of Hp; however, increasing doses to 300 mg Hp prevented necrotic tissue injury, while 900 mg Hp decreased necrotic as well as abnormal tissue regions, such that 53% ± 12% were of normal appearance and only 47% ± 13% were of abnormal appearance, with no necrotic regions observed.

*Timing of vascular tissue recovery*. In this nonlethal model, guinea pigs were otherwise normal and healthy absent the transfusion. After transfusion, in the vasculature, coagulative necrotic regions observed in the 28-day-old blood group developed collagen formation that accounted for 61% ± 9.8% of the aortic root by 48 hours after initial assessment. This was significantly different than collagen formation in the aortic root of animals transfused with new blood, 27% ± 5.0%, and those transfused with old blood plus Hp, 37% ± 9.0% (Figure 3, D and E).

*Renal proteomics — protein profiling of the predominant Hb clearance organ after blood transfusion*. Representative gross morphology images of kidneys 24 hours after transfusion with new blood, old blood, and old blood plus Hp are depicted (Figure 4, A–C). Animals transfused with new blood demonstrated normal gross morphology; conversely, animals transfused with old blood demonstrated consistent dark red and black discoloration, particularly within cortical regions (6 out of 6 animals transfused). Coinfusion of Hp with old-blood transfusion attenuated this effect, presumably by preventing renal decompartmentalization of Hb. We screened for quantitative protein changes related to Hb exposure/metabolism, oxidative stress, and parenchymal tissue injury 24

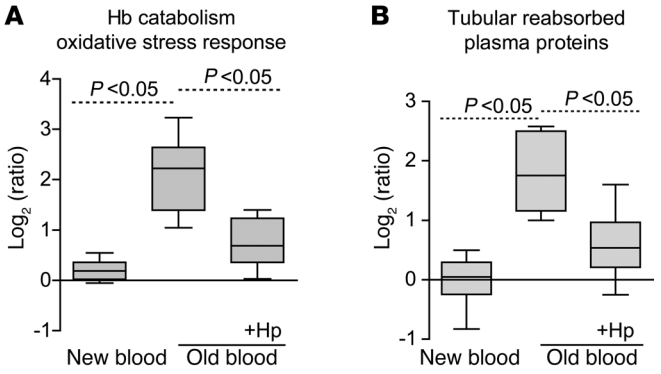


**Figure 5**
Renal tissue proteomic analysis. Quantifications of functional protein categories were extracted from Table 1 and summarized for the different transfusion groups. (**A**) Cumulative proteins in the category of Hb/heme catabolism and oxidative stress (defined by Nrf-2–activated proteins). (**B**) Proteins typically filtered and reabsorbed/degraded by renal tubulus cells. In each case, significant ($P < 0.05$) differences were observed among new blood, old blood, and old blood plus Hp with regard to the designated protein categories. Box plots represent 25%, 50%, and 75% percentiles, horizontal bars represent median values, and whiskers indicate minimum to maximum values.

hours after transfusion in kidneys. In 4 independent mass spectrometry experiments (with $n = 4$ animals per treatment group), we identified 1,554 proteins in at least 2 out of 4 experiments with a false discovery rate of less than 1% at peptide and less than 5% at the protein identification level. Quantitative estimates of protein abundances were derived from iTRAQ analysis. The graph in Figure 4D shows all the proteins that were identified in at least 2 out of 4 experiments. Each protein's relative abundance across the 3 treatment groups (compared with NTs) is shown as a single line. The superimposed box plots represent the fraction of proteins that were found to be overrepresented in the new and old blood (with or without Hp) groups. These data show that a number of proteins are overrepresented after transfusion with old blood, but not new blood, and that coadministration of Hp can attenuate these changes (Figure 4D).

The most extensively changed proteins are summarized in Table 1, and a complete list of the proteomic data is provided in Supplemental Table 1. We have manually screened the literature to assign the old blood–associated proteins to functional categories (Figure 5), in particular those related to Hb/heme metabolism, oxidative stress, and renal physiology/tubular reabsorption. Group differences in relative quantitation of Hb-α globin and Hb-β globin as well as Hb metabolic pathway proteins, such as heme oxygenase-1 (HO-1), biliverdin reductase B, and ferritin-heavy/light chains, were observed, indicating extensive heme exposure of the kidneys of animals transfused with old blood. Hp coinfusion with old blood attenuated accumulation of Hb-α globin and Hb-β globin and most heme-associated metabolic enzymes, while new-blood transfusion showed no changes in these protein levels. The potential impact of old-blood transfusion–associated Hb exposure on renal physiology is demonstrated by the accumulation of several plasma proteins that are typically reabsorbed and degraded by tubular epithelial cells (i.e., cystatin C). Hp coinfusion with old blood attenuated the increases in the accumulation of tubular reabsorbed proteins, while new-blood transfusion showed no changes in these protein levels (Figure 5).

*Hb release from stored rbc after transfusion contributes to renal pathology that is attenuated by Hp coinfusion*. Hb accumulation in the urine of animals transfused with old blood was observed after 24-hour collections; however, this was not observed in animals transfused with new blood or old blood plus Hp (Figure 6A). Renal exposure to Hb was further confirmed by tissue staining for iron accumulation, total renal iron, and globin chain tissue staining (Figure 6, B and C). Renal iron increased significantly ($P < 0.05$, old blood compared with new blood) at 24 hours after old-blood transfusion to 15.9 ± 2.4 μg per 100 mg tissue compared with 12.2 ± 0.92 μg per 100 mg tissue (new blood) and 13.4 ± 0.76 μg per 100 mg tissue (old blood plus Hp) (Figure 6D). The proteome pattern also indicated overabundance of some proteins that are controlled by the principle oxidative stress transcription factor Nrf-2, suggesting enhanced oxidative stress in the kidneys of animals transfused with old blood (Table 1, see noted Nrf-2–associated proteins). Immunofluorescence and Western blot analyses confirmed increased nuclear accumulation of Nrf-2 in renal tubules after old-blood transfusion and, to some extent, in animals transfused with old blood plus Hp compared with animals transfused with new blood and NTs (Figure 6, E and F). HO-1 expression after old-blood transfusion was 8-fold greater than that after new-blood transfusion and 2-fold greater than that after old blood plus Hp transfusion (Figure 6G). These data suggest that Hb/heme exposure is attenuated but not entirely blocked by Hp coinfusion. Together with the renal proteomic profiling data, these findings support the interpretation that Hb exposure and subsequent activation of metabolic, antioxidant, and circulatory protein accumulation are significantly enhanced in the old blood group compared with the old blood plus Hp and new blood group.

Renal histopathology of animals transfused with old blood revealed dilated proximal and distal tubules, consistent with nephrosis and tubular degeneration typically associated with tubular dysfunction (Figure 7A). Significant elevations in serum creatinine from NT levels (0.38 ± 0.019 mg/dl) to a 7-fold increase (3.13 ± 0.88 mg/dl) in the old blood group were observed at 24 hours. Serum creatinine in old blood plus Hp (0.45 ± 0.028 mg/dl) and new blood (0.44 ± 0.023 mg/dl) was unchanged from that in NTs (Figure 7C). Histopathological changes were not evident in the animals transfused with new blood or old blood plus Hp (Figure 7A).

*Timing of renal tissue recovery*. Renal cortical injury was rapid and robust after massive transfusion of 28-day-old blood. However, these acute changes also resolved after cessation of rbc hemolysis, reflecting the strong regenerative potential of the kidney in response to acute injury. In particular, renal proximal and distal tubular dilation returned toward normal appearance by 48 hours after initial assessment (Figure 7B), and serum creatinine decreased accordingly from 3.1 ± 0.88 mg/dl to 0.9 ± 0.24 mg/dl (Figure 7C). Taken together, these data suggest that Hb release from rbc can contribute to acute renal failure caused by massive transfusion of older stored blood and that Hp can function as an effective therapeutic to attenuate toxic responses to within a physiologically manageable range.

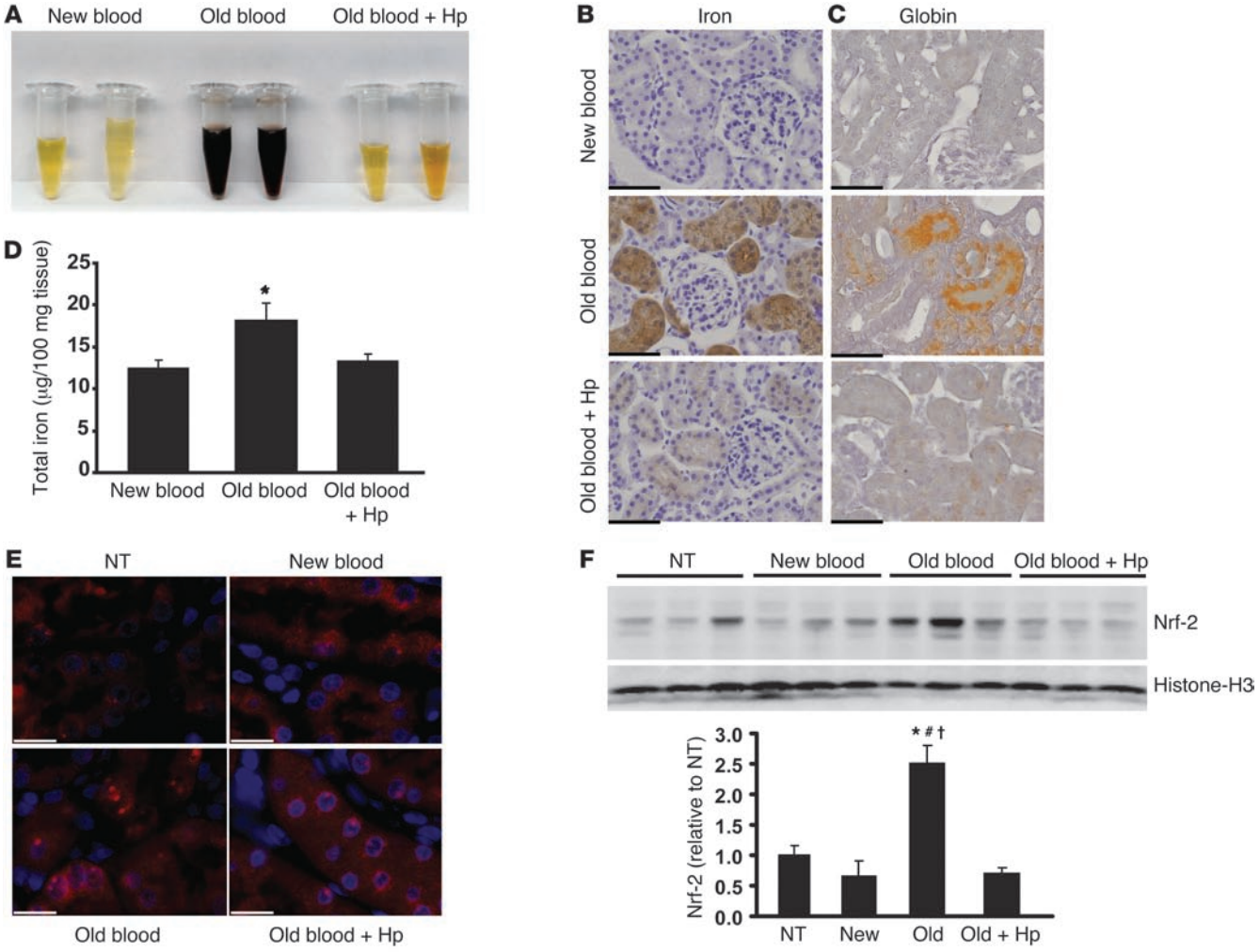


**Figure 6**

Renal Hb exposure, metabolic activation, and oxidative stress. (**A**) Twenty-four–hour urine collections show hemoglobinuria in the old blood group. (**B**) Perls iron staining demonstrates regions of iron accumulation, shown as brown, and granular effect in the old blood and, to some extent, old blood plus Hp groups (original magnification, ×400). (**C**) Okajima's staining for globin chain deposition after transfusions shows globin chain deposition as orange staining in the renal tubules (original magnification, ×400). (**D**) Tissue iron quantitation by the ferrozine method indicates a significant ($P < 0.05$) increase in total iron in kidneys after old blood transfusion compared with that after new blood transfusion. Iron after transfusion with new and old blood plus Hp did not differ from that in NTs. (**E**) Nrf-2 immunofluorescence at 24 hours after transfusion. Red immunofluorescence within Hoechst-stained blue nuclei indicates nuclear localization of Nrf-2 in old and to some extent old blood plus Hp. These observations were not observed in NTs or new blood–transfused animals kidneys (original magnification, ×600). (**F**) Nrf-2 nuclear Western blotting indicates a significant ($P < 0.05$) increase in nuclear Nrf-2 protein compared with that in NT, new blood, old blood plus Hp, and other transfusion groups. (**G**) HO-1 Western blotting indicates a significant increase in renal HO-1 after transfusion of old blood when compared with that of NTs and animals transfused with new blood and old blood plus Hp after 24 hours. Animals transfused with old blood plus Hp also demonstrated a significant increase ($P < 0.05$) in HO-1 relative to that in NTs and animals transfused with new blood. Scale bars (1 cm) = 25 μm (**B** and **C**); scale bars (6 mm) = 10 μm (**E**). *$P < 0.05$; #$P < 0.05$; †$P < 0.05$.

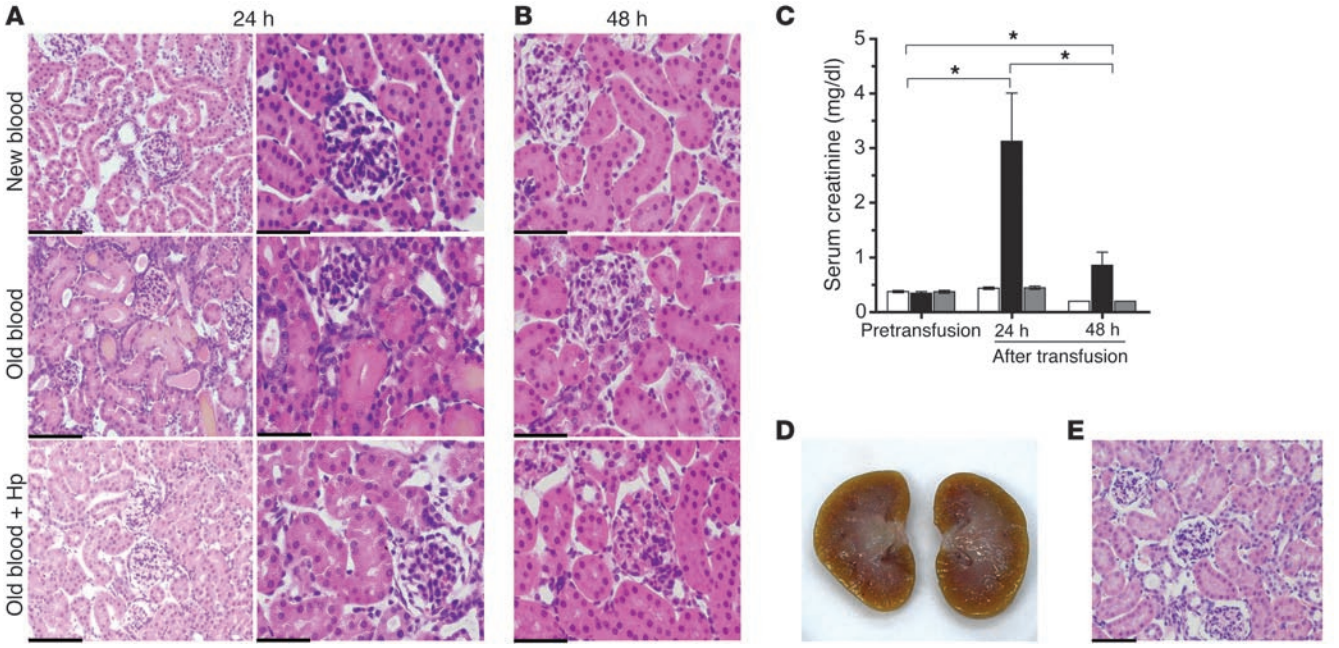


**Figure 7**
Renal tubular injury. (**A**) H&E-stained kidney tissue at 24 hours after transfusion shows new blood, old blood, and old blood plus Hp at 24 hours after transfusion. Old blood–transfused animal kidneys show distinct regions of proximal and distal tubular dilation and necrosis. These regions are not observed in new blood or old blood plus Hp groups (original magnification, ×200 [left]; ×400 [right]). (**B**) Recovery of tissue is observed in tissue 48 hours after transfusion (original magnification, ×400). (**C**) Histopathological events are reflected in serum creatinine, indicating a significant (*$P < 0.05$) increase 24 hours after old-blood transfusion compared with that after new and old blood plus Hp transfusion. The 48-hour recovery group showed a significant decline (*) in creatinine in serum creatinine. (**D** and **E**) The absence of gross and histopathological effects of bolus infusion of free Hb dosed to match the maximal plasma Hb concentration observed with old blood. Scale bars (1 cm) = 50 μm (**A**, left, and **E**); 25 μm (**A**, right, and **B**).

*Posttransfusion hemolysis, vascular, and renal effects of intermediate storage time rbc.* We additionally evaluated the effects of blood transfused after an intermediate storage period of 21 days (Figure 8). The exposure ($AUC_{0–24h}$) to extracellular Hb after 80% transfusion of 21-day-old blood was 865 ± 90 $\mu M \cdot h \cdot ml^{-1}$. This was approximately 5-fold less than the 24-hour Hb exposure after 28-day-old blood transfusion but significantly greater than Hb exposure after new-blood transfusion (Figure 8A), and 24-hour renal excretion of Hb remained evident (Figure 8B). H&E staining of aortic root tissue 24 hours after transfusion (Figure 8C) indicated that 21-day-old blood transfusion resulted in significant damage. The areas of abnormal and necrotic appearing tissue were similar with 28-day-old blood and were also found to be associated with iron accumulation in the adventitia (Figure 8C). The effect of renal Hb clearance noted in 24-hour urine collections demonstrated the same extent of renal cortical iron deposition compared with that in 28-day-old blood (Figure 8E, bottom). Renal iron per 100 mg of tissue was significantly greater in the kidneys transfused with 21-day-old blood (15.9 ± 1.9 ng/100 mg tissue) and 28-day-old blood (17.5 ± 0.71 ng/100 mg tissue) than in those after new-blood transfusion (9.5 ± 1.2 ng/mg tissue) kidneys (Figure 8F). However, in contrast to transfusion of 28-day-old blood, which results in acute kidney failure, these changes appeared to represent subclinical findings, since serum creatinine was unchanged from basal levels in the group transfused with blood stored for 21 days (data not shown).

In summary, the cumulative Hb exposure and tissue damage found after transfusion of blood stored for 21 days was significant compared with that after new-blood transfusion but less severe than the changes observed after old blood (28 days storage) transfusion. Therefore, a storage time–dependent component appears to contribute to the blood transfusion–associated adverse effects in our model.

*The impact of in vivo (after transfusion) versus in vitro (before transfusion) hemolysis.* As shown in Figure 1, a small fraction of rbc do undergo hemolysis during storage, and in vitro hemolysis within the storage bag has previously been proposed as a possible factor in the pathophysiology associated with stored-blood transfusion (16). We have therefore performed 2 sets of experiments to dissect the contribution of in vitro (before transfusion) versus in vivo (after transfusion) hemolysis in our model.

A group of animals were dosed with a bolus infusion of purified guinea pig Hb to match the peak plasma heme concentration (approximately 300 μM) achieved after old-blood transfusion. Since we found supernatant storage solution typically contained low Hb concentrations after 28 days of storage, this experiment mimics a hypothetical condition to test the effects of Hb resulting from severe in vitro hemolysis occurring in a storage bag. Results demonstrated no remarkable changes to gross vascular and renal morphology or histopathology previously shown (Figure 7, D and E). Additionally, no temporal changes were observed in serum creatinine levels in these animals (data not shown). These results suggest preinfusion hemolysis is not a predominant cause of the tissue damage observed in our old-blood transfusion model.

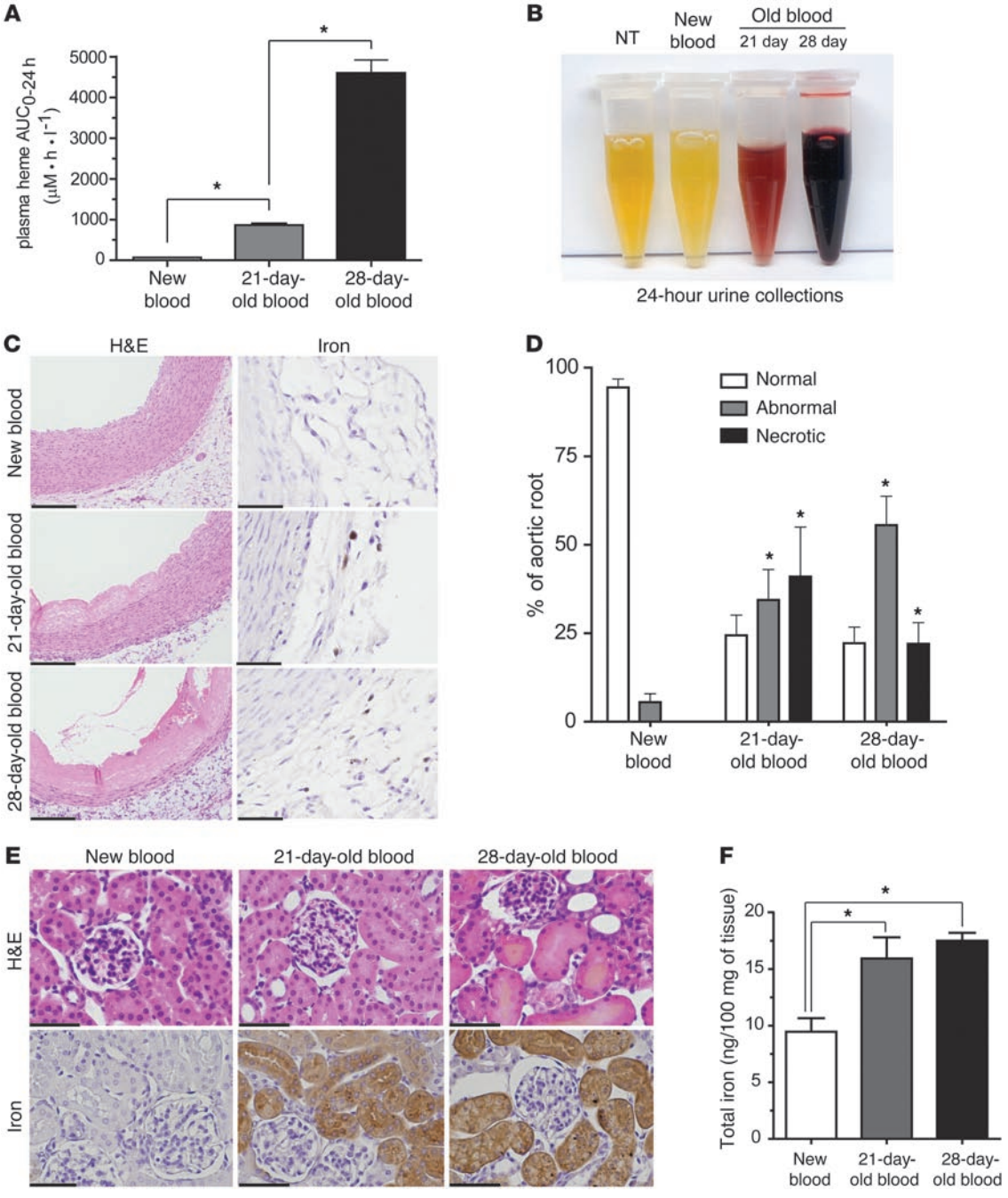


**Figure 8**

Cardiorenal response to 21-day-old blood transfusion. (**A**) Hb exposure over 24 hours, derived from plasma concentration versus time data as area under the curve ($AUC_{0–24}$), shows significantly increased Hb exposure after transfusion with 21-day-old and 28-day-old blood compared with that with new blood. (**B**) The 24-hour urinary Hb excretion after transfusion in guinea pigs. (**C**) H&E staining of aortic tissue, showing coagulative necrosis in the 21-day-old and 28-day-old blood transfusion groups (original magnification, ×400 [left]). Iron staining of aortic root showing new blood, 21-day-old blood, and 28-day-old blood transfusion groups (original magnification, ×600 [right]). (**D**) Percentage of normal, abnormal, and necrotic aortic root. Significantly increased abnormal and necrotic regions were observed with transfusion of 21-day-old and 28-day-old blood compared with that with new blood. (**E**) Iron deposition is shown as brown stained and granular areas. H&E-stained renal cortex in the 3 transfusion groups. Dilated proximal and distal tubules can be seen as swollen tubules with irregular shape, orange-colored casts, and irregular distribution of nuclei after 28-day-old blood transfusion. Perls iron stained renal cortex in the 3 transfusion groups. Original magnification, ×400. Iron deposition is shown as brown stained and granular areas. (**F**) Iron deposition showing ng iron per 100 mg tissue. 21-day-old blood and 28-day-old blood showed significantly greater iron deposition than new blood. Scale bars (1 cm) = 25 μm (**C**, H&E, and **E**); scale bars (6 mm) = 10 μm (**C**, iron). *$P < 0.05$.

In another set of experiments, washed 28-day-old blood was transfused and resulted in a plasma Hb $AUC_{0-24h}$ of 2,045 ± 369 $\mu M \cdot h \cdot ml^{-1}$. This value was approximately 2-fold less than the Hb exposure after nonwashed 28-day-old blood transfusion (Figure 9A). The pooled post-wash supernatant (6 total washes, final wash was clear) is shown as an inset in Figure 9B. Importantly, serial ektacytometry analysis of rbc before and after the washing procedure shows an increase in deformability. Prior to transfusion (i.e., after PBS washing) the cell population was more deformable than the original old blood, suggesting that the repeated cycles of centrifugation and resuspension removed both extracellular Hb and some Hb from nondeformable cells (Figure 9B). This observation is likely a result of mechanical destruction of the most fragile rbc during the wash procedure and indicates that experiments with washed rbc may in fact underestimate the true level of in vivo hemolysis after transfusion of nonwashed old blood. The 24-hour blood sample obtained from transfused guinea pigs ($n$ = 4) demonstrated rbc with normal deformability. Aortic root changes after transfusion of 28-day-old washed blood are shown in Figure 9C. Tissue morphology within the aortic root demonstrated similar changes as those found after nonwashed old-blood transfusion (Figure 9D). The gross morphology of kidneys after transfusion with washed 28-day-old blood showed a darkened renal cortex (Figure 9E). Renal iron per 100 mg of tissue was significantly greater in the kidneys after transfusion with washed 28-day-old blood (19 ± 2.2 ng/100 mg tissue) and the 28-day-old nonwashed blood (17.5 ± 0.71 ng/100 mg tissue) when compared with new-blood transfusion (9.5 ± 1.2 ng/100 mg tissue) kidneys (Figure 9G). Histopathology of renal cortical tissue revealed abnormal morphology of proximal and distal tubules; however, tissue was absent of dilated tubules observed after nonwashed 28-day-old blood transfusion (Figure 9F, top). Compatible with the less severe morphologic changes after washed old-blood transfusion, we did not detect significant changes in posttransfusion creatinine levels.

In summary, these 2 sets of experiments suggest that the 2 components of in vitro and in vivo hemolysis may both contribute to the cumulative pathophysiology of stored-blood transfusion. However, bolus exposure to free Hb that could accumulate in the storage bag is apparently not sufficient to induce gross pathologic changes. In contrast, transfusion of washed rbc can mimic the general pattern of pathology observed after large-volume transfusion of old blood, even though a significant loss of fragile rbc does occur during the washing procedure and may limit correct estimations of in vivo hemolysis upon old-blood transfusion. Therefore, we assume that in vivo posttransfusion hemolysis is the main component responsible for tissue Hb exposure and pathology in our model.

## Discussion

This study was designed based on multiple published retrospective clinical analyses that suggested poor outcome after transfusion of older storage blood and is intended to be iterative in providing mechanistic insight into these observations. Understanding pathophysiological factors is highly relevant to understanding triggers for adverse outcomes and to identify ways to prevent acute and longer-term pathologies with specific therapeutic interventions. Previous work suggests that altered biochemistry of stored rbc can modify various rbc membrane functions and these modifications collectively lead to the storage lesion (32, 33). However, a cohesive description of the impact of the rbc storage lesion in vivo is lacking. We hypothesized that the storage time–dependent structural change of rbc may lead to in vivo intravascular hemolysis after transfusion. Adverse physiology is subsequently mediated by Hb exposure and occurs via acute vascular dysregulation (e.g., hypertension) and oxidative events. Importantly, the decrease in deformability, which was assumed in our study as a surrogate marker of rbc structural changes of older storage guinea pig rbc, approximates that in human rbc stored under similar blood banking conditions for the maximum currently allowed storage period. The decreased deformability may be directly related to intravascular hemolysis. However, other important mechanisms of rbc destruction may be relevant. For example, senescent rbc destruction resulting from erythrophagocytosis has been shown to increase Hb and iron after transfusion of as little a 1 unit of older storage blood in human volunteers (34). This may be caused by storage-related cell surface exposed phosphatidylserine (35) and may become more significant in patients receiving larger volumes of blood. Another potential contributor may be associated with anti–band 3 antibodies that ultimately activate complement and can lead to rbc phagocytosis (22). A critical distinction between small- and large-volume transfusion is that extravascular hemolysis can extend to intravascular hemolysis, as observed in this study. The consequences of in vivo hemolysis in our model were identified as tissue changes that are indicative of acute endothelial dysfunction, vascular damage, and early organ failure in the kidney.

Cardiovascular effects of extracellular Hb have been extensively studied in the context of hemolytic diseases and Hb-based oxygen carrier administration and are reported in the literature with regard to (transient, but occasionally severe) hypertension and myocardial injury (20, 26, 27). In agreement with these data, our studies demonstrate an acute and transient rise in systemic blood pressure after transfusion of old blood. We previously demonstrated that Hp has the unique capacity to neutralize the hypertensive activity of Hb infusions in dogs and guinea pigs (20). Therefore, the observation that sequestration of Hb within a Hb-Hp complex could also block the hypertensive activity of old-blood transfusion implies that Hb release from senescent rbc likely accounts for this observation in the present model. However, other processes, such as excessive release of rbc arginase (which would deplete the NO synthase substrate arginine), may act as additional factors independent of Hb-mediated effects. In our model, Hb-dependent NO consumption by plasma from animals transfused with old blood conforms to the most extensively investigated concept of hemolysis mediated vascular dysfunction (13, 14). In contrast, the protective effect of Hp can not be explained by a simple biochemical mechanism whereby systemic NO depletion would be attenuated by altered NO reactivity of the complex. In contrast, the evident dissociation of hypertension/vascular damage and NO consumption that was observed on a systemic level suggests that Hp rather helps to preserve local NO signaling within critical microenvironments such as the vascular wall. This effect could be related to a molecular size–dependent compartmentalization effect that strictly restrains the biochemical reactivity of the large Hb-Hp complex within the circulation. Therefore, it remains to be thoroughly investigated whether the molecular size of the Hb-Hp complex shifts the location of NO scavenging and other activities out of the subendothelial or extraglomerular space. Important to this concept are previous experiments that suggest Hp can effectively restrict transendothelial diffusion of extracellular Hb (36). Furthermore, NO-independent effects such as enhanced control of Hb's oxidative reactivity within the complex may be relevant in our transfusion model.

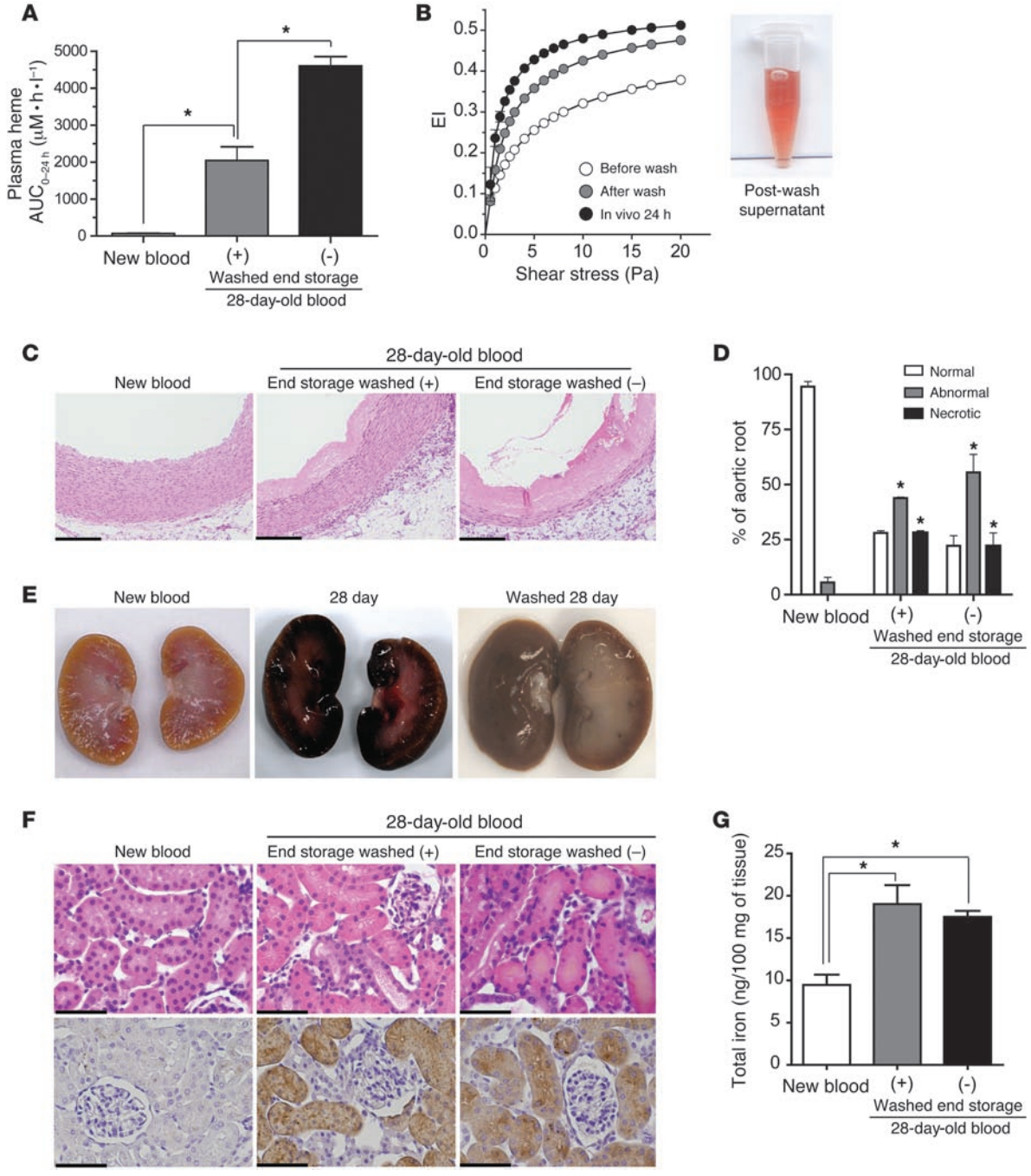


**Figure 9**

Cardiorenal response to 28-day-old blood transfusion before and after washing. (**A**) Hb exposure over 24 hours ($AUC_{0–24}$) demonstrated significantly greater Hb exposure after transfusion of 28-day-old blood (with washing) and 28-day-old blood (without [–] washing) compared with that after new blood. (**B**) The EI of rbc stored for 28 days and measured before and after washes with PBS as well as the EI of blood sampled from guinea pigs at 24 hours after transfusion ($n = 4$ guinea pigs). The image shows supernatant from 6 washes of 28-day-old rbc. (**C**) H&E staining of aortic root tissue showing coagulative necrosis in the (washed) 28-day-old blood and (unwashed) 28-day-old blood transfusion groups. Original magnification, ×400. (**D**) Percentage of normal, abnormal, and necrotic aortic root. Significantly increased abnormal and necrotic regions were observed with transfusion of washed 28-day-old blood and (unwashed) 28-day-old blood compared with new blood. (**E**) Gross morphology images of kidneys after transfusion of new blood and 28-day-old blood before and after washing. (**F**) H&E-stained renal cortex. Dilated proximal and distal tubules can be seen as tubules with irregular shape, orange-colored casts, and irregular distribution of nuclei. Perls iron staining is shown as brown granular structures in tubules. Original magnification, ×400. (**G**) Iron deposition as ng iron per 100 mg tissue. Significantly greater iron deposition versus new blood. Scale bars (1 cm) = 25 μm (**C** and **F**). *$P < 0.05$.

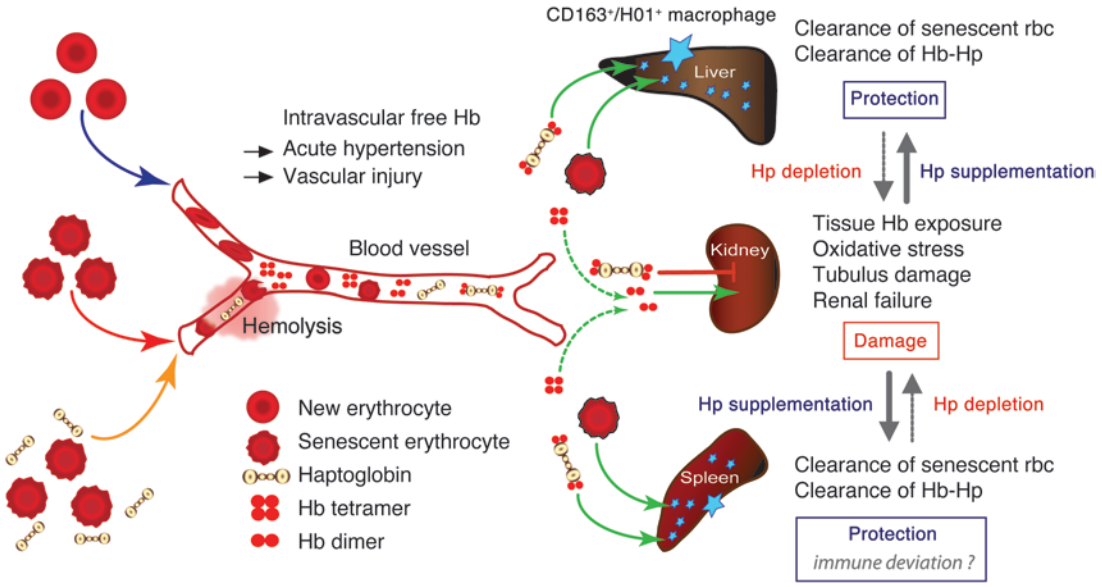


**Figure 10**
Schematic summary of experimental observations and a proposed mechanistic pathway. The hypothesis of hemolysis as a major contributor to storage lesion toxicity–associated older storage blood is outlined. This process is hypothesized to be driven by increased rigidity of older storage rbc coupled with large-volume transfusion. In the circulatory compartment, this leads to Hb-associated vascular effects, such as hypertension and direct vascular injury. In high clearance extravascular compartments such as the kidney, injury is driven by Hb exposure, oxidative stress, and acute/chronic renal failure. Hp supplementation via coinfusion with older blood transfusion can (a) prevent renal filtration and (b) redirect clearance to liver and spleen for removal by macrophages. In the circulation, Hp may effectively limit Hb interaction with the vascular wall.

We additionally evaluated the root of the aortic arch after new blood and old blood with or without Hp transfusion. To our knowledge, this study is the first to evaluate large vessel abnormalities associated with sustained Hb exposure after rbc transfusion. Vascular wall injury and perivascular accumulation of iron, HO-1, and CD163-positive macrophages were prominent after old-blood transfusion. In contrast to the transient hypertensive response, vascular damage did not resolve within the first 48 hours after transfusion but was associated with significant collagen deposition within the vessel wall. This observation suggests more chronic and potentially persistent vascular remodeling. Again, vascular injury was not observed with new-blood transfusion and attenuated when Hp was coinfused with old blood, thus lending evidence to hemolysis-driven pathophysiology. The sequence of events leading to these changes may involve a mutual interaction of Hb-mediated oxidative stress, local NO depletion, vasa vasorum damage, endothelial injury, and acute hypertension. These findings might be particularly relevant given that one of the largest clinical studies on old blood–related adverse effects examined cardiac surgery patients. Most of these patients had preexisting cardiovascular pathologies and might therefore be particularly vulnerable to the cardiovascular toxicity of old blood (1).

The kidneys are the primary route of Hb clearance after depletion of endogenous Hp. The kidneys are therefore highly susceptible to organ dysfunction resulting from hemolysis (37) and potentially after stored rbc transfusion. Initial gross morphology and proteomic profiling data from animals transfused with old blood indicated both Hb exposure and adaptive responses typically controlled by the prototypic oxidative stress transcription factor Nrf-2. Besides a typical Hb/heme exposure and oxidative stress protein signature in the kidneys of animals transfused with old blood, our proteome-wide tissue profiling approach identified intrarenal accumulation of a number of plasma proteins that are typically reabsorbed and degraded by renal tubular cells. Taken together with the absence of albumin accumulation (that would be expected in case of overt glomerular damage), these findings suggest distorted renal tubular function as a primary mechanism of global renal impairment. Further exploration of renal tissue demonstrated renal tubular dilation consistent with nephrosis and, in some cases, renal tubular degeneration and necrosis in animals transfused with old blood. The renal damage and functional impairment after old-blood transfusion was following an acute course with delayed recovery. These findings were not observed after new-blood transfusion and could be prevented by Hp coinfusion. While Hp effectively prevented the deleterious consequences of vascular and kidney exposure to Hb, it apparently did not interfere with physiologic sequestration and clearance of senescent rbc. Comparable erythrophagocytosis and heme-driven HO-1 responses could be observed in liver and spleen macrophages in animals transfused with old blood with or without Hp (Supplemental Figure 1). Importantly, we could rule out the potential for decreased tissue oxygenation as a causative factor in the observed tissue injury (see Supplemental Results and Supplemental Figures 2 and 3).

In conclusion, the present study design allowed us to define the in vivo result of the blood storage lesion after massive transfusion. A clear sequence of events was observed that included enhanced rbc deformability in vitro, intravascular hemolysis after transfusion, and subsequent Hb-mediated pathophysiology within different tissue compartments. This pathophysiol-

ogy seems to be determined by a storage time–dependent component, as suggested by the gradual increase of hemolysis and damage with transfusion of new blood, intermediate storage period blood, and old blood. A model for this hypothesis based on our experimental findings is summarized in Figure 10. The coadministration of the natural Hb scavenger Hp served a dual role in this model. (a) Due to the highly specific and well-characterized Hb-neutralizing activity of Hp, we could unequivocally identify Hb as a distinct and quantitatively important factor in transfusion-induced pathological changes, and (b) Hp coadministration with older storage blood could therefore be an effective countermeasure to reduce stored-blood transfusion–associated pathologies, particularly in cardiovascular compromised and critically ill patients or those receiving multiple or massive blood transfusions.

## Methods

*Materials, animal, and surgical preparation*. A detailed description of materials, animals, and anesthetic and surgical procedures as well as blood collection and storage protocols is provided in the Supplemental Methods.

*Blood collection and storage*. Blood was collected from guinea pigs under anesthesia using an aseptic technique via a left carotid artery catheter into CPDA-1–filled syringes (Baxter Healthcare Inc.). Collections were pooled (approximately 20 ml × 10 donor animals) and leukocyte reduced using a neonatal High Efficiency Leukocyte Reduction Filter and storage bag (Purecell Neo, Pall Corporation) supplemented with additive solution (AS-3, Pall Corporation). The final preservative concentration was equal to 14%, and bags were maintained in the dark at 4°C over a 28-day period. Human rbc were purchased from the Swiss Red Cross Blood Bank, collected from donors in CPDA-1, and leukocyte reduced for storage in saline-adenine-glucose-mannitol additive solution (42-day storage rated) according to standard Swiss Red Cross blood banking protocol for comparison purposes (Swiss Red Cross; written informed consent was obtained from all donors in accordance with the Declaration of Helsinki), as described previously (38). For comparison of rbc deformability, human rbc and guinea pig rbc were stored in 42-day approved storage solutions. Human rbc were collected in SAG-M, and guinea pig rbc were collected in AS-3 (according to our approved protocols). No differences were observed following in vivo rbc viability with these 2 solutions based on labeling studies (39). Comparative deformability data on stored human and guinea pig rbc are provided to prove that our guinea pig model of stored rbc transfusion was within a range of what could reasonably be expected with human rbc that were stored under approved blood banking conditions.

*Transfusion protocol*. Twenty-four hours after recovery from surgical catheter implantation, guinea pigs were transfused with (a) new blood (2-day storage), (b) old blood (28-day storage), or (c) old blood with 750 mg Hp coinfusion. A detailed protocol of blood collection, rbc preparation, and storage conditions is given in the Supplemental Methods. Endogenous blood was withdrawn at 5-minute intervals via the arterial catheter, and new blood, old blood, and old blood with 750 mg Hp were infused at a rate of 0.25 ml/min via the venous catheter. Exchanges were performed using separate syringe pumps (model 11, Harvard Apparatus) connected to arterial and venous catheters and were carried out until 80% of each guinea pig's blood volume was replaced. Determination of blood volume was estimated for each animal according to the following equation: blood volume (ml) = (0.07 [ml/g] × body weight [g]) × 0.8 in the guinea pig (40). In a separate group of animals, stroma-free guinea pig Hb was infused to achieve a maximum concentration ($C_{max}$ = 300 μM) comparable to that observed with animals transfused with old blood for the purpose of assessing acute Hb exposure effects on pathophysiology. Sham controls (NTs) underwent surgical preparation without transfusion.

*rbc deformability and analysis of free and intracellular Hb*. The detailed protocol for osmotic gradient ektacytometry using laser diffraction (RheoScan-D, RheoMeditech) and Hb measurement (in vitro and in vivo) is given in the Supplemental Methods. The extent of Hb binding to Hp was measured by size-exclusion chromatography on a BioSep-SEC-S3000 column (600 mm × 7.5 mm, Phenomenex) attached to a Waters 2535 Quaternary Gradient Module and 2948 Photodiode Array Detector (Waters Corporation).

*Renal tissue proteomic analysis*. Evaluation of kidneys was performed as a screening method to identify protein categories of interest. A detailed description of tissue preparation for proteomic analysis can be found in the Supplemental Methods. Briefly, kidneys were excised and cut transversely to separate cortex and medulla. The cortex was subjected to homogenization, trichloroacetic acid protein precipitation, trypsin digestion, reducing/blocking of digests, and iTRAQ sample labeling (performed according to the manufacture instructions; Applied Biosystems). Mass spectrometry analysis was performed on an LTQ Orbitrap Velos (Thermo Scientific). A more detailed description of methodology is provided in the Supplemental Methods.

*Tissue pathology and Hb exposure*. Protocols for tissue preparation/fixation and (immuno)histochemistry are provided in the Supplemental Methods.

*Statistics*. All data are presented as mean ± standard error of the mean. Significance between groups was determined based on planned comparisons using a 1-way ANOVA. A posteriori Bonferroni's test was performed to determine difference between groups and baseline (GraphPad Prism, version 5). A $P$ value of less than 0.05 was considered to be statistically significant. Studies evaluated 6 animals per group, with the exception of proteomic profiling, for which 3 animals were evaluated.

*Study approval*. The animal protocol (no. 2009-25) for male Hartley guinea pigs was approved by the FDA/CBER Institutional Animal Care and Use Committee, with all experimental procedures performed in adherence to the NIH guidelines on the use of experimental animals. Human rbc were obtained for research purposes (Swiss Red Cross). Written informed consent was obtained from all donors in accordance with the Declaration of Helsinki, and research with these blood products was approved by the ethics committee of the Kanton of Zurich (38).

## Acknowledgments

This work was supported by FDA Critical Path Funding (to P.W. Buehler and F. D'Agnillo), Swiss National Science Foundation (grant 31003A_138500) (to D.J. Schaer), and by the University of Zurich Research Priority Program "Integrative Human Physiology" (to D.J. Schaer and P.W. Buehler). The authors would like to thank Francine Wood for oxygen equilibrium measurements. The findings and conclusions in this article have not been formally disseminated by the FDA and should not be construed to represent any agency determination or policy.

Received for publication June 30, 2011, and accepted in revised form February 8, 2012.

Address correspondence to: Paul W. Buehler, CBER, FDA, 8800 Rockville Pike, Bldg. 29, Rm. 129, Bethesda, Maryland 20892, USA. Phone: 301.451.3953; Fax: 301.435.4034; E-mail: paul.buehler@fda.hhs.gov. Or to: Dominik J. Schaer, Division of Internal Medicine, University Hospital, CH-8091 Zurich, Switzerland. Phone: 41.44.255.2382; Fax: 41.44.255.8517; E-mail: dominik.schaer@usz.ch.

1. Koch CG, et al. Duration of red-cell storage and complications after cardiac surgery. *N Engl J Med*. 2008;358(12):1229–1239.
2. Purdy FR, Tweeddale MG, Merrick PM. Association of mortality with age of blood transfused in septic ICU patients. *Can J Anaesth*. 1997;44(12):1256–1261.
3. Zallen G, et al. Age of transfused blood is an independent risk factor for postinjury multiple organ failure. *Am J Surg*. 1999;178(6):570–572.
4. Donaldson MD, Seaman MJ, Park GR. Massive blood transfusion. *Br J Anaesth*. 1992;69(6):621–630.
5. Haradin AR, Weed RI, Reed CF. Changes in physical properties of stored erythrocytes relationship to survival in vivo. *Transfusion*. 1969;9(5):229–237.
6. Gilson CR, et al. A novel mouse model of red blood cell storage and posttransfusion in vivo survival. *Transfusion*. 2009;49(8):1546–1553.
7. Hendrickson JE, et al. Rapid clearance of transfused murine red blood cells is associated with recipient cytokine storm and enhanced alloimmunogenicity. *Transfusion*. 2011;51(11):2445–2454.
8. Hod EA, et al. Transfusion of red blood cells after prolonged storage produces harmful effects that are mediated by iron and inflammation. *Blood*. 2010;115(21):4284–4292.
9. Fitzgerald RD, Martin CM, Dietz GE, Doig GS, Potter RF, Sibbald WJ. Transfusing red blood cells stored in citrate phosphate dextrose adenine-1 for 28 days fails to improve tissue oxygenation in rats. *Crit Care Med*. 1997;25(5):726–732.
10. Simchon S, Jan KM, Chien S. Influence of reduced red cell deformability on regional blood flow. *Am J Physiol*. 1987;253(4 pt 2):H898–H903.
11. Hill A, et al. Eculizumab prevents intravascular hemolysis in patients with paroxysmal nocturnal hemoglobinuria and unmasks low-level extravascular hemolysis occurring through C3 opsonization. *Haematologica*. 2010;95(4):567–573.
12. Pamplona A, et al. Heme oxygenase-1 and carbon monoxide suppress the pathogenesis of experimental cerebral malaria. *Nat Med*. 2007;13(6):703–710.
13. Minneci PC, et al. Hemolysis-associated endothelial dysfunction mediated by accelerated NO inactivation by decompartmentalized oxyhemoglobin. *J Clin Invest*. 2005;115(12):3409–3417.
14. Reiter CD, et al. Cell-free hemoglobin limits nitric oxide bioavailability in sickle-cell disease. *Nat Med*. 2002;8(12):1383–1389.
15. Rother RP, Bell L, Hillmen P, Gladwin MT. The clinical sequelae of intravascular hemolysis and extracellular plasma hemoglobin: a novel mechanism of human disease. *JAMA*. 2005;293(13):1653–1662.
16. Donadee C, et al. Nitric oxide scavenging by red blood cell microparticles and cell-free hemoglobin as a mechanism for the red cell storage lesion. *Circulation*. 2010;124(4):465–476.
17. Kim-Shapiro DB, Lee J, Gladwin MT. Storage lesion: role of red blood cell breakdown. *Transfusion*. 2011;51(4):844–851.
18. Nishiyama T, Hanaoka K. Free hemoglobin concentrations in patients receiving massive blood transfusion during emergency surgery for trauma. *Can J Anaesth*. 2000;47(9):881–885.
19. Zager RA, Gamelin LM. Pathogenetic mechanisms in experimental hemoglobinuric acute renal failure. *Am J Physiol*. 1989;256(3 pt 2):F446–455.
20. Boretti FS, et al. Sequestration of extracellular hemoglobin within a haptoglobin complex decreases its hypertensive and oxidative effects in dogs and guinea pigs. *J Clin Invest*. 2009;119(8):2271–2280.
21. Auerbach HS, Burger R, Dodds A, Colten HR. Molecular basis of complement C3 deficiency in guinea pigs. *J Clin Invest*. 1990;86(1):96–106.
22. Giger U, Sticher B, Naef R, Burger R, Lutz HU. Naturally occurring human anti-band 3 autoantibodies accelerate clearance of erythrocytes in guinea pigs. *Blood*. 1995;85(7):1920–1928.
23. Bunn HF. Differences in the interaction of 2,3-diphosphoglycerate with certain mammalian hemoglobins. *Science*. 1971;172(3987):1049–1050.
24. Buehler PW, D'Agnillo F, Hoffman V, Alayash AI. Effects of endogenous ascorbate on oxidation, oxygenation, and toxicokinetics of cell-free modified hemoglobin after exchange transfusion in rat and guinea pig. *J Pharmacol Exp Ther*. 2007;323(1):49–60.
25. Butt OI, Buehler PW, D'Agnillo F. Differential induction of renal heme oxygenase and ferritin in ascorbate and nonascorbate producing species transfused with modified cell-free hemoglobin. *Antioxid Redox Signal*. 2010;12(2):199–208.
26. Yu B, Raher MJ, Volpato GP, Bloch KD, Ichinose F, Zapol WM. Inhaled nitric oxide enables artificial blood transfusion without hypertension. *Circulation*. 2008;117(15):1982–1990.
27. Burhop K, Gordon D, Estep T. Review of hemoglobin-induced myocardial lesions. *Artif Cells Blood Substit Immobil Biotechnol*. 2004;32(3):353–374.
28. Frei AC, et al. Vascular dysfunction in a murine model of severe hemolysis. *Blood*. 2008;112(2):398–405.
29. Yeo TW, et al. Relationship of cell-free hemoglobin to impaired endothelial nitric oxide bioavailability and perfusion in severe falciparum malaria. *J Infect Dis*. 2009;200(10):1522–1529.
30. Salazar Vazquez BY, Cabrales P, Tsai AG, Johnson PC, Intaglietta M. Lowering of blood pressure by increasing hematocrit with non nitric oxide scavenging red blood cells. *Am J Respir Cell Mol Biol*. 2008;38(2):135–142.
31. Sharma VS, Traylor TG, Gardiner R, Mizukami H. Reaction of nitric oxide with heme proteins and model compounds of hemoglobin. *Biochemistry*. 1987;26(13):3837–3843.
32. Dern RJ, Brewer GJ, Wiorkowski JJ. Studies on the preservation of human blood. II. The relationship of erythrocyte adenosine triphosphate levels and other in vitro measures to red cell storageability. *J Lab Clin Med*. 1967;69(6):968–978.
33. Greenwalt TJ, Bryan DJ, Dumaswala UJ. Erythrocyte membrane vesiculation and changes in membrane composition during storage in citrate-phosphate-dextrose-adenine-1. *Vox Sang*. 1984; 47(4):261–270.
34. Hod EA, et al. Transfusion of human volunteers with older, stored red blood cells produces extravascular hemolysis and circulating non-transferrin-bound iron. *Blood*. 2011;118(25):6675–6682.
35. Bosman GJ, Cluitmans JC, Groenen YA, Werre JM, Willekens FL, Novotny VM. Susceptibility to hyperosmotic stress-induced phosphatidylserine exposure increases during red blood cell storage. *Transfusion*. 2011;51(5):1072–1078.
36. Nakai K, et al. Permeability characteristics of hemoglobin derivatives across cultured endothelial cell monolayers. *J Lab Clin Med*. 1998;132(4):313–319.
37. Ohshiro TU, Mukai K, Kosaki G. Prevention of hemoglobinuria by administration of haptoglobin. *Res Exp Med (Berl)*. 1980;177(1):1–12.
38. Schaer DJ, et al. CD163 is the macrophage scavenger receptor for native and chemically modified hemoglobins in the absence of haptoglobin. *Blood*. 2006;107(1):373–380.
39. Hillyer CD, ed. *Blood Banking And Transfusion Medicine, Basic Principles And Practice*. Philadelphia, Pennsylvania, USA: Elsevier; 2007:186–187.
40. Ancill RJ. The blood volume of the normal guinea-pig. *J Physiol*. 1956;132(3):469–475.